ARTICLE

Polymeric Memory Elements and Logic Circuits that Store Multiple Bit States

Graham de Ruiter,[†] Yair H. Wijsboom,[†] Noa Oded,[‡] and Milko E. van der Boom*[,†]

Department of Organic Chemistry and Applied Mathematics and Computer Science, The Weizmann Institute of Science, 76100 Rehovot, Israel

ABSTRACT The ever-increasing flow of information requires new approaches for high-density data storage (HDDS). Here, we present a novel solution that incorporates the easily accessible polymer poly(3,4-ethylenedioxythiophene) (PEDOT) with multistate memory. The electrical addressable polymer is able to store up to five different memory states, which are stable up to 20 min. The observed memory states are generated by the optical output signature of the PEDOT deposited on indium tin oxide (ITO) coated glass, upon applying specific electrical inputs. Moreover, the demonstrated platforms can be represented by a general logic circuit, which allows the construction of multistate memory, such as flip-flops and flip-flap-flop logic circuits.

KEYWORDS: sequential logic • molecular memory • reconfigurable • functional integration • thin films

1. INTRODUCTION

As early as 1943, it was realized that relays in the first digital computing devices were actually analogous to the functioning of neurons and that they could be imitated by telegraph relays and vacuum tubes (1). The functioning of the nervous system was even analyzed in terms of propositional logic (2). The use of molecules in bottom-up schemes, therefore, might be an attractive approach for solving (upcoming) problems in information processing and storage (3). However, this realization took another 50 years to materialize, when it was discovered, that molecules could perform mathematical operations, and thereby mimic the in- and output characteristics of electronic circuitry (4). Henceforth, the field of molecular logic has made significant advances and many logic gates and circuits have been demonstrated (5−7), which are fundamental in computer design (8). In particular, the formation of organic memory elements is currently of great interest (9). Ideally, the next generation of memory elements should be capable of (i) high-density data storage (HDDS), (ii) fast access time, (iii) operating at low potentials, and (iv) storing data for prolonged periods of time.

High-density data storage is of major importance, in order to cope with the ever-increasing amount of information. As a result, many new nanostructured materials including (organic) molecules (9a, 9c), inorganic nanowires (10), and polymeric materials (11) have been explored as suitable memory devices. To date, almost exclusively, binary memory is involved. As suggested, by us and others, an alternative method is to increase the number of available memory states (12).

Scheme 1. Molecular Structure of the Poly(3,4-ethylene-dioxythiopene) (PEDOT) Coated on ITO Employed in This Study

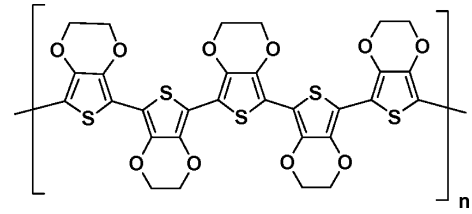

Electrochromic materials are suitable candidates, for the formation of multistate memory as recently reported (12a). In this regard, π-conjugated polymers are attractive, since the absorbance can be controlled upon applying different potential biases (13). For instance, the absorbance intensity of the readily available polymer poly(3,4-ethylenedioxythiophene) (PEDOT; Scheme 1) can be systematically varied by applying different potentials between −0.9 and 1.0 V, whereupon the color switches from dark blue in the undoped state to transparent gray in the doped state (Figure S1 and Scheme S1, Supporting Information) (13).

Moreover, such electrochromic polymers are inexpensive, easy to fabricate and/or process, highly customizable, robust and work at low potential biases, which make them suitable for fabricating devices (14). Therefore, such materials can be applied in thin film transistors (OTFTs) (15), light-emitting diodes (OLEDs) (16), electrochromic displays (ECDs) (17), electrochromic windows (18), and photovoltaic cells (19). However, their use as multistate static random access memory (SRAM), which employs the conventional flip-flop architecture, has rarely been addressed. Only a few examples can be found that suggest multilevel data storage in a dynamic random access memory (DRAM)-like fashion (20).

* To whom correspondence should be addressed. E-mail: milko.vanderboom@weizmann.ac.il.

Received for review August 17, 2010 and accepted November 10, 2010

[†] Department of Organic Chemistry.

[‡] Applied Mathematics and Computer Science.

DOI: 10.1021/am1007497

Published on Web 11/29/2010

Here, we demonstrate, for the first time, that the conductive polymer PEDOT deposited on indium tin oxide (ITO) coated glass can be used for generating multistate SRAM that is able to store up to five different states with retention times up to 20 min (21). This enabled us to store binary, ternary, quaternary, and quinary digits on a polymer-based film in a reversible and reconfigurable way. Interestingly, this memory can be represented by sequential logic circuits that have multiple parallel cross-coupled set/reset (SR) latches, such as the flip-flop and the flip-flap-flop. Each successive increase of one memory state results in the functional integration of one cross-coupled NOR gate into the circuit. The demonstrated retention times are equivalent to retention times that are reported for volatile memory (10a, 11a). Moreover, the read and write operations are fundamentally different: optical and electrochemical, respectively. The optical readout is nondestructive and allows instantaneous data transfer and results in increased durability of the memory.

2. EXPERIMENTAL SECTION

2.1. Materials and Methods. The PEDOT-coated indium tin oxide (ITO) substrates were produced by electrochemical deposition from solution by a previously reported procedure (13a). In short, PEDOT was deposited on ITO (working electrode) from of a solution of 3,4-ethylenedioxythiophene (EDOT) in acetonitrile with 0.1 M tetrabutylammonium tetrafluoroborate ($TBABF_4$) as the supporting electrolyte upon applying a potential of 1.3 V (vs Ag/AgCl) until a charge of 10 mC was reached. Single-side indium tin oxide (ITO)-coated float glass substrates (8−12 Ω) were purchased from Delta Technologies (Stillwater, MN) and were cleaned by rinsing with acetone and alcohol. UV/vis spectra were recorded on a Cary 100 spectrophotometer between 200 and 800 nm. $TBABF_4$ was purchased from Sigma Aldrich and recrystallized twice from H_2O before use. Electrochemical measurements were performed on a CHI 660A potentiostat with ITO, platinum, and Ag/AgCl as a working, counter, and reference electrode, respectively. All measurements were carried out in acetonitrile with $TBABF_4$ (0.1 M) as electrolyte in the multipotential chronoamperometric mode at 298 K unless stated otherwise.

2.2. General Experimental Setup. A typical experimental setup is as follows: a platinum wire and Ag/AgCl are used as a counter and reference electrode, respectively. The working electrode is the PEDOT-coated ITO. The experiment is conducted in the multipotential chronoamperometric mode with $TBABF_4$ (0.1 M) in acetonitrile as the electrolyte. The chronoamperometric mode allows successive potentials to be set for a specific amount of time, with a desired number of potential sweeps (cycles), after which the potentiostat will turn off the potential automatically. When the potential is turned off, the condition is reached, in which all potentials are absent (for example, input string; 0 0 0). Note that only one connection to the ITO is needed because the potentials are not allowed to be active at the same time. In this way, it is possible to use just one wire to apply the three different potential values.

2.3. Optical Properties of the PEDOT-Coated ITO as a Function of the Potential. The PEDOT-coated ITO was oxidized and reduced by applying double-potential steps, with 1 s intervals, between −0.60 V and $(-0.60 + n0.05)$ V with $n = 1-24$. Monitoring the band at $\lambda = 630$ nm resulted in accurate control over the transparency of the PEDOT-coated film, since the ΔA ($A_{ox} - A_{red}$) is a precise function of the voltage until full oxidation is achieved. Upon applying a potential between −0.60 and 0.60 V, the PEDOT switches from the undoped state (dark blue) to the doped state (transparent gray).

2.4. Absorbance Switching between Multiple Potential Segments. The PEDOT-coated ITO was partially oxidized and reduced by switching the electrochemical potential between segmented values. For instance, the absorbance was split into two regions by applying a double-potential step, with 1 s intervals, between −0.60 and −0.01 and between −0.01 and 0.60 V, respectively. This resulted in two distinct regions of absorption values that are highly reproducible. In addition, the absorption values can further be divided into 3, 4, and 5 regions, by segmenting the electrochemical potential accordingly.

2.5. Multistate Memory with PEDOT-Coated ITO. In the multipotential chronoamperometric mode, different memory states can be generated by applying consecutive electrochemical potentials for 3 s, with subsequent monitoring of the absorbance band at $\lambda = 630$ nm. For example, two different memory states can be generated by applying a potential of −0.60 and 0.60 for 3 s, in a consecutive order. This was further utilized to demonstrate three (−0.60, 0.00, and 0.60 V), four (−0.60, −0.10, 0.15, and 0.60 V) and five (−0.60, −0.15, 0.00, 0.15, and 0.60 V) memory states. This results in a reproducible platform that is capable of generating binary, ternary, quaternary, and quinary digits. The response time of the PEDOT-coated ITO was calculated by analyzing how much time it takes to switch between the different states generated by the different potential values (see Supporting Information).

2.6. 2-State Retention Time of the PEDOT-Coated ITO. The bit retention time of the PEDOT-coated ITO was investigated by applying double-potential steps, with 3 s intervals, between −0.60 and 0.60 V, in order to demonstrate reversibility. Thereafter, the evolution of the absorbance band at $\lambda = 630$ nm was monitored as a function of time, in the absence of any potential. This experiment was repeated two times with −0.60 and 0.60 V as final potential pulse. Before each experiment, the electrolyte solution was purged with nitrogen for 20 min, and during the experiment, a nitrogen flow was maintained above the electrochemical cell. However, small amounts of doping of the PEDOT was observed, manifested by small traces of oxygen present in the solution, as indicated by a 21% decrease in absorbance after 25 min. Similarly, a small amount (17%) of undoping was observed after oxidation of the PEDOT-coated ITO.

2.7. 3-State Retention Time of the PEDOT-Coated ITO. The trit retention time of the PEDOT-coated ITO was investigated by applying a triple-potential step, with 3 s intervals, between 0.60, 0.00, and −0.60 V, in order to demonstrate reversibility. Thereafter, the evolution of the absorbance band at $\lambda = 630$ nm was monitored as a function of time, in the absence of any potential. This experiment was repeated three times with 0.60, 0.00, and −0.60 V as final potential pulse. Before each experiment, the electrolyte solution was purged with nitrogen for 20 min, and during the experiment, a nitrogen flow was maintained above the electrochemical cell. After oxidation of the PEDOT-coated ITO, a 7% increase in absorbance was observed. In contrast, a 25% decrease in the absorbance was observed after the polymer was undoped. The state obtained after applying a potential of 0.00 V is remarkably stable.

2.8. Multiple-State Retention Times of the PEDOT-Coated ITO. The multiple-bit retention times of the PEDOT-coated ITO were investigated by applying a triple-potential step, with 3 s intervals, between 0.60, −0.60, and X Volt, where X is the potential that generates the memory state ($X = -0.10$, 0.00, 0.10., 0.25, and 0.60 V, respectively). After this short cycle was used to demonstrate reversibility, the evolution of the absorbance band at $\lambda = 630$ nm was monitored as a function of time. Before each experiment, the electrolyte solution was purged with nitrogen for 20 min, and during the experiment, a nitrogen flow was maintained above the electrochemical cell. Since five different potentials were used to generate the different states,

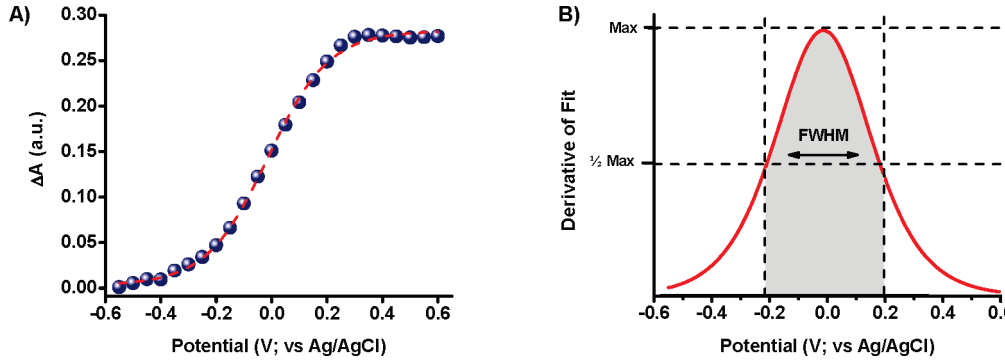

FIGURE 1. Optical properties of the PEDOT-coated ITO. (A) Optical response (ΔA; $A_{red} - A_{ox}$) of the absorbance band, at $\lambda = 630$ nm, as a function of the voltage. The dashed red line is a sigmoidal fit ($R^2 = 0.997$), with an inflection point at −0.02 V. (B) Derivative of the sigmoidal fit and the corresponding full-width at half-maximum (FWHM).

the obtained data can be arranged in any order to create the "multistate" memory. In this way, the quaternary and quinary memory were generated.

2.9. Reproducibility of the Retention Time of the PEDOT-Coated ITO. The reproducibility of retention time of the PEDOT-coated ITO was investigated by applying a triple-potential step, with 3 s intervals, between 0.60, 0.00, and −0.60 and between 0.60, 0.25, and −0.16 V to test the reproducibility of the memory states in the multistate memory. After these short cycles, the evolution of the absorbance band at $\lambda = 630$ nm was monitored as a function of time. This procedure was repeated five times for each state. Before each experiment, the electrolyte solution was purged with nitrogen for 20 min, and during the experiment, a nitrogen flow was maintained above the electrochemical cell. Note that this data is not normalized and gives a small drift in the observed absorbance spectra.

3. RESULTS AND DISCUSSION

As previously reported, it is important to realize that although the (doped or undoped) PEDOT is inherently bistable, multiple regions can be generated by addressing the assembly as a whole (Figure S2, Supporting Information) (12a). Therefore, one can use the optical output at $\lambda = 630$ nm of the PEDOT-coated ITO to store the multivalued information, since this is a precise function of the applied potential (Figures 1A and S1, Supporting Information) (20b). In this particular case, the output is defined as the ΔA; that describes the absorbance difference between the undoped state (A_{red}) and the partially doped state (A_{ox}) of the PEDOT-coated ITO. The sigmoidal shape of this function is important; differentiation of the sigmoidal fit will produce a normal distribution centered on the $E_{1/2}$ of the polymer (Figure 1B). In this regard, the full-width at half-maximum (FWHM) is crucial: A small FWHM value will reduce the number of attainable memory states since the optical output is very sensitive toward small changes in the applied potential. In contrast, a large FWHM value enables one to store many memory states; however, it requires a broad potential range. This might be undesirable, as it can lead to an operation potential, which is impractical with which to work. In addition, the FWHM also influences the accuracy of the inputs; a small deviation of the input potential will cause a large error in the optical output. Obviously, there is a trade-off between the desired amount of memory states and the required potential range. For the PEDOT-coated ITO, the FWHM spans 0.4 V (from −0.20 to 0.20 V), which is excellent for generating several memory states (vide infra). Together with an operating potential between −0.60 and 0.60 V, the PEDOT-coated ITO is an ideal platform for storing information, at low power consumption.

In the following experiments, the presence of an applied potential is defined as a logical 1, whereas a logical 0 is defined as the absence of the applied potential (open circuit condition). The writing of the data occurs when a certain potential is applied, which results in a change in absorption. The data are subsequently read as the optical output at $\lambda = 630$ nm of the PEDOT-coated ITO on glass, which allows for a nondestructive read-out. Finally, each state can be overwritten by applying a different potential. To prevent contradicting outputs of our memory device, only one input can be active at the same time (8).

The above-mentioned principles can be used to mimic binary latching (flip-flop) memory. Applying a potential pulse of −0.60 V (logical 1; input I_1) results in the undoping of the PEDOT film and a concurrent increase in the absorbance value of the band at $\lambda = 630$ nm (state 1). In contrast, applying a potential pulse of 0.60 V (logical 0; input I_N) results in doping of the PEDOT-coated ITO film, which subsequently bleaches the band at $\lambda = 630$ nm (state 0). The concomitant doping and undoping upon applying a series of potential pulses is illustrated in Figure 2A. The switching time between the undoped (1) and doped state (0) of the memory is around 500 ms (see Supporting Information, Figure S3). Most importantly, for completion of the set/reset (SR) flip-flop, it is essential that the memory should be stable under open circuit conditions. This was investigated by applying a double-potential step between −0.60 and 0.60 V, with either −0.60 or 0.60 V as the final potential pulse. Thereafter, the evolution of the absorbance band at $\lambda = 630$ nm was monitored as a function of time, in the absence of any potential (Figures 4A and S4A−D, Supporting Information). As indicated, the stability of state 1 (undoped) is high, although some decrease in absorption is observed due to doping of the PEDOT, as manifested by the presence of trace amounts of oxygen. The stability of state 0 (doped) under open circuit conditions is similar. Therefore, this system can be best described by an SR flip-flop (Figure 7; input I_1 and I_N), with a retention time of 25 min for both states 1 and 0.

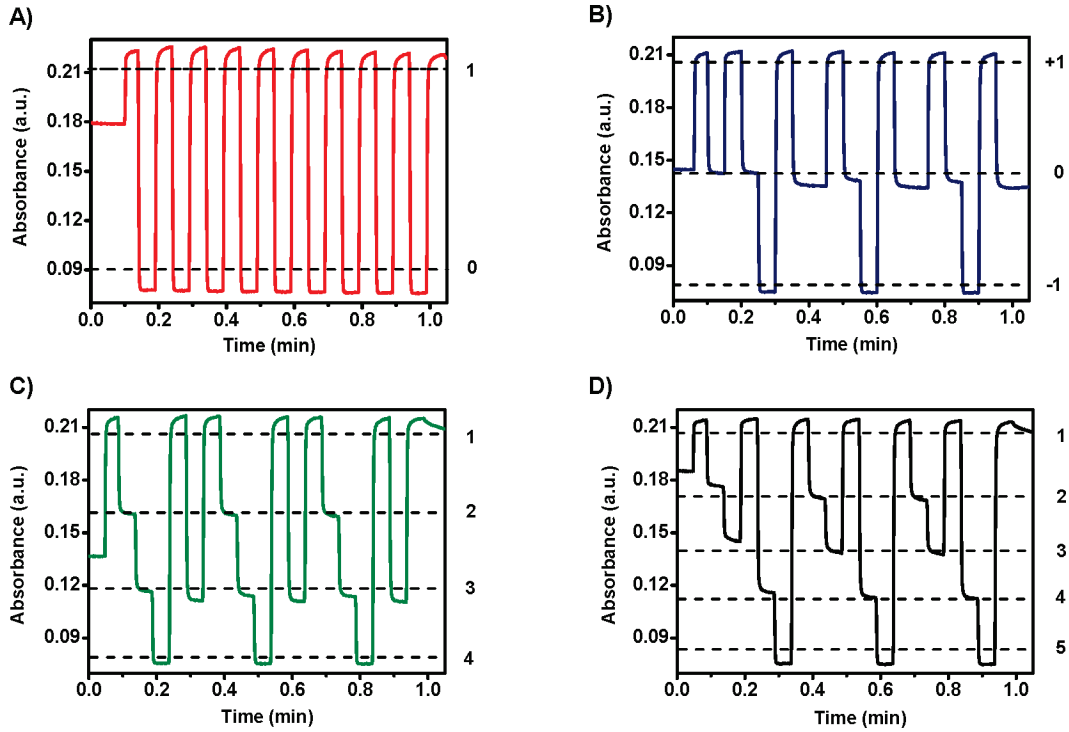

FIGURE 2. Multiple absorbance states of the PEDOT coated ITO. Optical response of the absorbance band at $\lambda = 630$ nm of the PEDOT-coated ITO as a function of time, upon applying different multipotential steps with 3 s intervals. (A) Double-potential steps between −0.60 and 0.60 V. (B) Triple-potential steps between −0.60, 0.00, and 0.60 V. (C) Quadruple-potential steps between −0.60, −0.10, 0.15, and 0.60 V. (D) Quintuple-potential steps between −0.60, −0.15, 0.00, 0.15, and 0.60 V.

Although the generation of binary memory is well explored (the PEDOT is bistable), the formation of ternary memory is not. Exploration of ternary memory is desirable, since it is expected that the flip-flap-flop architecture will eventually replace the flip-flop in SRAM (22). In addition, base three is also the most efficient system for information processing (23). Since the PEDOT exhibits low signal-to-noise ratios and combines high stability with good control over the optical properties, the generation of balanced ternary memory devices is possible. For example, three different absorption states can be generated by choosing −0.60, 0.00, and 0.60 V as the applied input potentials (Figure 2B). Applying a potential of −0.60 V (input I_1) results in full undoping of the PEDOT (Figure 2B) and the system being in state +1. However, applying a potential of 0.00 V (Input I_2) results in a partially doped film, and the system is in state 0. State −1 can be generated by applying a potential of 0.60 V (input I_N). On average, the switching time between states takes 350 ms, whereas switching between two states takes around 500 ms. Moreover, the generated ternary memory exhibits excellent retention times, where the three different states can be clearly distinguished, even after 25 min (Figures 4B and S5A−F, Supporting Information). This behavior is summarized in the characteristics presented in Table 1 and in the corresponding flip-flap-flop logic circuit (Figure 7; inputs I_1, I_2, and I_N with $N = 3$).

The aforementioned examples of binary and ternary memory are considered the most important, since they are closely related to conventional systems. However, if only data storage is considered, it does not necessarily have to be limited to three states. In general, the more states that

Table 1. General Characteristics Table for Multistate Memory

#	Inputs				Output	
	I_1	I_2	···	I_N	AB···*N*	Overall
1	0	0	···	0	Store State	
2	1	0	···	0	10···0	1
3	0	1	···	0	01···0	2
⋮	⋮	⋮	⋮	⋮	⋮	⋮
N_{+1}	0	0	···	1	00···1	*N*

can be generated, the higher the information density will become (Figure 3), and fewer amount of digits are required to represent a given number (22, 24). An additional problem

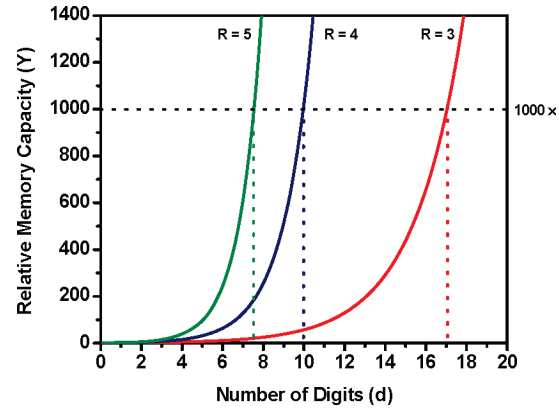

FIGURE 3. Relative memory increase, compared to binary memory, by increasing the number of memory states (R), for $R = 2$, 3, 4, and 5.

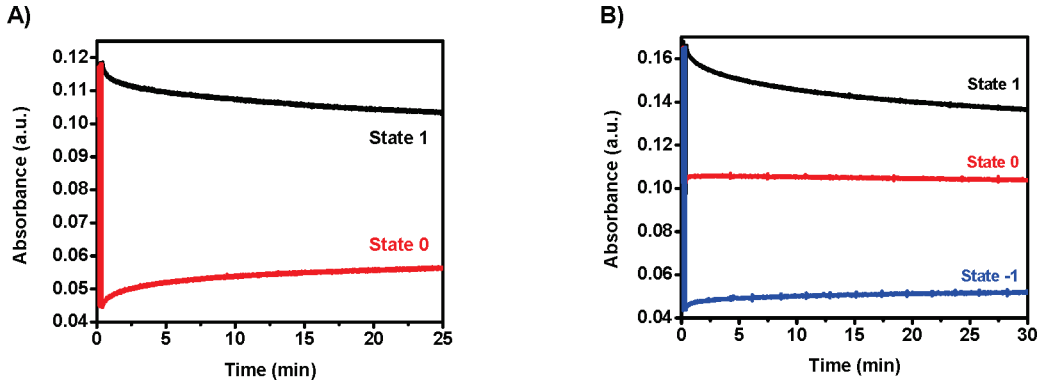

FIGURE 4. Retention times of the binary and ternary memory. Evolution of the absorbance at $\lambda = 630$ nm of the PEDOT-coated ITO, as a function of time upon applying a multipotential step with 3 s intervals. (A) Binary memory generated by applying a double-potential step between −0.60 and 0.60 V with −0.60 V as the final pulse (black trace) and 0.60 as the final pulse (red trace). (B) Ternary memory generated by applying a triple-potential step between −0.60, 0.00, and X V, where X denotes the final pulse that generates the memory state. X = −0.60 V as the final pulse (black trace); $X = 0.00$ V as the final pulse (red trace), and $X = 0.60$ V as the final pulse (blue trace).

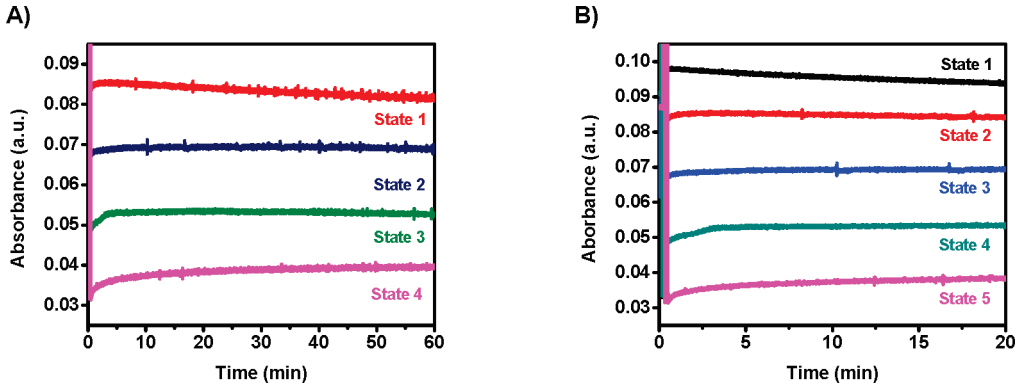

FIGURE 5. Retention times of the quaternary and quinary memory. Evolution of the absorbance at $\lambda = 630$ nm of the PEDOT-coated ITO, as a function of time upon applying a multipotential step with 3 s intervals (A) Quaternary memory generated by applying a triple-potential step between −0.60, 0.00, and X V, where X denotes the final pulse that generates the memory state. $X = 0.00$ V (red trace); $X = 0.10$ V (blue trace); $X = 0.25$ V (green trace), and $X = 0.60$ V (magenta trace). (B) Quinary memory generated by applying a triple-potential step between −0.60, 0.60, and X V, where X denotes the final pulse that generates the memory state. $X = -0.10$ V (black trace); $X = 0.00$ V (red trace); X = 0.10 V (blue trace); $X = 0.25$ V (green trace), and $X = 0.60$ (magenta trace).

is that the individual states need to be distinguished accurately in order to prevent scrambling of the internal memory.

In this sense, the FWHM of the PEDOT-coated ITO allows the formation of stable memory that can store four and five different states. For instance, as a representative example, four different absorption states can be generated by applying a continuous potential of −0.60, −0.10, 0.15, or 0.60 V, respectively (Figure 2C). Similarly, applying a continuous potential of −0.60, −0.15, 0.00, 0.15, or 0.60 V results in the formation of five different absorption states (Figure 2D). As long as the potential is applied, the states are easily distinguished. However, under open-circuit conditions, the states cannot be easily distinguished anymore due to the auto-oxidation of the PEDOT by O_2. For the binary and ternary memory states, this is not a problem, since the ΔA is sufficiently large. In order to create four- and five-state memory, however, different potentials should be chosen, because the full potential range is not appropriate. Close inspection of Figure 4B indicates that the memory states generated by potentials >0.00 V are highly stable. Therefore, in order to achieve high retention times for four- and five-state memory, it is better to choose the input potentials between 0.00 and 0.60 V. For example, five different potentials can be chosen to generate five individual states that are stable up to 60 min (Figure S6A−J, Supporting Information). Although, working with a smaller potential window reduces the ΔA between each state, the individual memory states have been stabilized. As a consequence, any of those five potentials can be chosen to create multistate memory. Although this includes binary and ternary memory, only for the four- and five-state memory, this does have a clear advantage. Indeed, when the input potentials are defined as follows: 0.00 V (input I_1), 0.10 V (input I_2), 0.25 V (input I_3), and 0.60 V (input I_N), four stable memory states can be generated (Figure 5A). Even after 60 min, the four states can be easily distinguished.

In terms of molecular logic, we have generated two-, three- and four-memory states that can be represented by cross-coupling NOR logic gates. The general logic circuits consist of interconnected OR logic gates, whose function is to select and distribute the proper inputs for the cross-coupled NOR gates (Figure 7). Any multistate memory can be demonstrated that function with I_N inputs, where N is the number of states. In our case, $N = 2$, 3, 4, or 5 to generate binary, ternary, quaternary, and quinary memory, respectively. It is important to realize that each subsequent addition of one memory state unto the memory (N increases by 1)

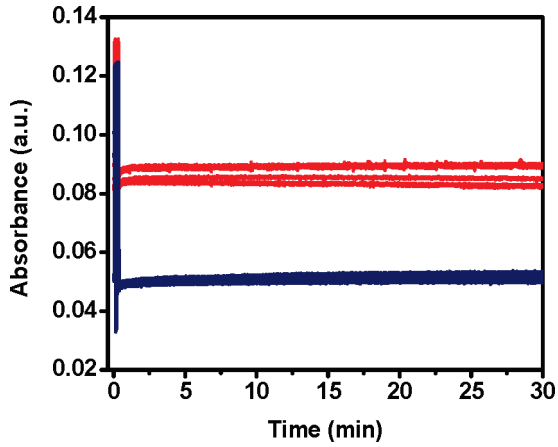

FIGURE 6. Reproducibility of the memory states after five consecutive read/write/erase cycles upon applying a triple-potential step for 3 s and subsequent monitoring of the evolution of the absorption band at $\lambda = 630$ nm. (i) Triple-potential step between −0.60, −0.10, and 0.60 V with 0.00 V as the final potential pulse (state 1; red traces). (ii) Triple-potential step between −0.60, 0.25, and 0.60 V with 0.25 V as the final potential pulse (state 3; blue traces).

leads to the functional integration of one extra OR and one extra cross-coupled NOR gate into the logic circuit. This functional integration underlies the power of molecular logic (25), since a single assembly can mimic a complex integrated circuit with many logic gates, without the physical realization as such.

Similarly, for the formation of stable five-state memory, the following input potentials could be used: −0.10 V (input I_1), 0.00 V (input I_2), 0.10 V (input I_3), 0.25 V (input I_4), and 0.60 V (input I_N). Although the retention times are not as high, 25 vs 60 min for the four-state memory, it is still possible to clearly differentiate five stable states (Figure 5B). This type of memory is equivalent to a five-input latching circuit that consists of five cross-coupled NOR gates (Table 1 and Figure 7; $N = 5$) that operates according to the inputs in characteristics Table 1. Note that, since we are dealing with volatile memory (SRAM is volatile) (8), the reported retention times in this study are excellent and are approaching the retention times reported for state-of-the-art nonvolatile memory (10a, 11a).

We demonstrated here that the PEDOT-coated ITO is capable of differentiating up to five different memory states and that it is able to store four states with retention times up to 60 min. Upon applying a potential, the optical properties can be reversed and are with great stability. However, memory devices should also be able to store the information accurately and reproducibly without scrambling the internal memory states after each write/erase cycle. The reproducibility of retention times of the PEDOT-coated ITO was investigated by applying a triple-potential step, with 3 s intervals, between 0.60, 0.00, and −0.60 V and between 0.60, 0.25, and −060 V to test the reproducibility of the generated states. After these short cycles, the evolution of the absorbance band at $\lambda = 630$ nm was monitored as a function of time (Figure 6). This indicated that each memory state is highly reproducible. Even after 30 min, the values only have a standard deviation of 4% compared with the mean value.

The herein reported PEDOT-coated ITO out performs our layer-by-layer assembly consisting of osmium polypyridyl complexes cross-linked with $PdCl_2$ (12a). The FWHM of the molecule-based assembly is 0.17 V (from 0.85 to 1.02 V), which makes operability more complicated, since the optical output is sensitive toward small variations in the input potential. Although the switching times are somewhat slower for the PEDOT-coated ITO (500 vs 180 ms), we are now able to store four and five states in a static random access memory-like fashion, which was not possible before. Interestingly, the retention times of the generated memory states with the PEDOT-coated ITO are several orders of magnitude larger than for the molecule-based assembly. Moreover, it was recently shown that PEDOT could successfully be integrated for binary write-once read-many-times (WORM) memory devices (26). Our findings may expand

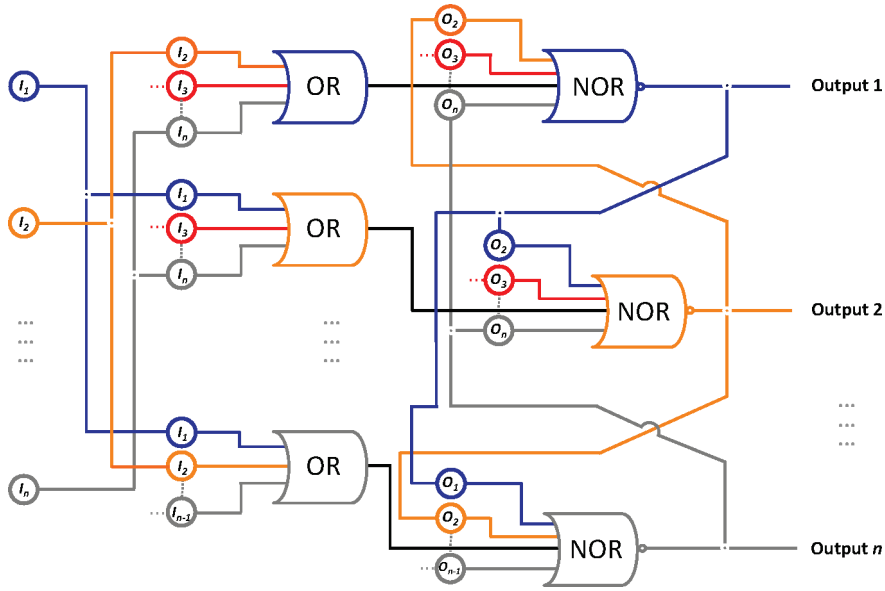

FIGURE 7. Generalized memory circuit capable of storing up to *N* different states in a single setup.

the scope of memory devices generated by such materials that can be written/read many times in a multistate fashion.

4. CONCLUSION

In conclusion, we have shown that the properties of PEDOT such as good ON/OFF ratios, high stability, and excellent FWHM can be utilized for fabricating memory elements that can store multivalued digits in a single assembly. Interstate switching times are moderate to fast and are dependent on the number of states. Moreover, the function of the memory can easily be reconfigured just by changing the number of input potentials. Interestingly, these memory functions can be represented by highly complex logic circuits in the form of cross-coupled NOR gates (flip-flops). Each successive addition of one memory state leads to the functional integration of one extra cross-coupled NOR gate into the circuit. This functional integration of logic gates underscores the importance of molecular logic, since it allows the mimicking of whole integrated circuits without the physical realization. In addition, the optical read-out is instantaneous and nondestructive. Moreover, it was recently reported that the redox-active assemblies on solid support could be used for the formation of an entirely electrical flip-flops (27). The easy access and the availability of established procedures for integrating this polymer into solid-state devices makes it an attractive candidate for HDDS that is entirely electrical.

Acknowledgment. This research was supported by the Helen and Martin Kimmel Center for Molecular Design, the Israel Science Foundation (ISF), and the Gerhardt M. J. Schmidt Minerva Center on Supramolecular Architectures.

Supporting Information Available: Experimental procedures and figures of absorbance of PEDOT-coated ITO, oxidation (p-doping) of the poly(3,4-ethylenedioxythiopene) or PEDOT, absorbance at $\lambda = 630$ nm of the PEDOT-coated ITO, response time of the binary memory, and retention times of the absorbance at $\lambda = 630$ nm of the PEDOT-coated ITO. This material is available free of charge via the Internet at http://pubs.acs.org.

REFERENCES AND NOTES

(1) von Neumann, J. *IEEE Ann. Hist. Comput.* **1993**, *15*, 27.
(2) McCulloch, W. S.; Pitts, W. *Bull. Math. Biophys.* **1943**, *5*, 115.
(3) Lieber, C. M. *Sci. Am.* **2001**, *285*, 50.
(4) de Silva, A. P.; Gunaratne, H. Q. N.; McCoy, C. P. *Nature* **1993**, *364*, 42.
(5) (a) Pischel, U. *Aust. J. Chem.* **2010**, *63*, 148. (b) Andreasson, J.; Pischel, U. *Chem. Soc. Rev.* **2010**, *39*, 174. (c) Szacilowski, K. *Chem. Rev.* **2008**, *108*, 3481. (d) Credi, A. *Angew. Chem., Int. Ed.* **2007**, *46*, 5472. (e) de Silva, A. P.; Uchiyama, S. *Nat. Nanotechnol.* **2007**, *2*, 399.
(6) (a) Liu, Y.; Offenhäusser, A.; Mayer, D. *Angew. Chem., Int. Ed.* **2010**, *49*, 2595. (b) Chung, J. W.; Yoon, S. J.; Lim, S. Y.; An, B. K.; Park, S. Y. *Angew. Chem., Int. Ed.* **2009**, *48*, 7030. (c) Mu, L.; Shi, W.; She, G.; Chang, J. C.; Lee, S. T. *Angew. Chem., Int. Ed.* **2009**, *48*, 3469. (d) Komatsu, H.; Matsumoto, S.; Tamaru, S.; Kaneko, K.; Ikeda, M.; Hamachi, I. *J. Am. Chem. Soc.* **2009**, *131*, 5580. (e) Gupta, T.; van der Boom, M. E. *Angew. Chem., Int. Ed.* **2008**, *47*, 5322. (f) Cheng, P. N.; Chiang, P. T.; Chiu, S. H. *Chem. Commun.* **2005**, 1285. (g) Guo, X. F.; Zhang, D. Q.; Zhu, D. B. *Adv. Mater.* **2004**, *16*, 125. (h) Szacilowski, K. *Chem.—Eur. J.* **2004**, *10*, 2520.
(7) (a) Amelia, A.; Baroncini, M.; Credi, A. *Angew. Chem., Int. Ed.* **2008**, *47*, 6240. (b) Andreasson, J.; Straight, S. D.; Moore, T. A.; Moore, A. L.; Gust, D. *J. Am. Chem. Soc.* **2008**, *130*, 1112. (c) Andreasson, J.; Straight, S. D.; Bandyopadhyay, S.; Mitchell, R. H.; Moore, T. A.; Moore, A. L.; Gust, D. *Angew. Chem., Int. Ed.* **2007**, *46*, 958. (d) Margulies, D.; Melman, G.; Shanzer, A. *Nat. Mater.* **2005**, *4*, 768. (e) Langford, S. J.; Yann, T. *J. Am. Chem. Soc.* **2003**, *125*, 11198. (f) de Silva, A. P.; McClenaghan, N. D. *J. Am. Chem. Soc.* **2000**, *122*, 3965.
(8) Mano, M. M.; Kime, C. R. In *Logic and Computer Design Fundamentals*, 4th ed.; Prentice Hall: Upper Saddle River, NJ, 2000.
(9) (a) de Ruiter, G.; Tartakovsky, E.; Oded, N.; van der Boom, M. E. *Angew. Chem., Int. Ed.* **2010**, *49*, 169. (b) Karnbratt, J.; Hammarson, M.; Li, S. M.; Anderson, H. L.; Albinsson, B.; Andreasson, J. *Angew. Chem., Int. Ed.* **2010**, *49*, 1854. (c) Periyasamy, G.; Collin, J. P.; Sauvage, J. P.; Levine, R. D.; Remacle, F. *Chem.—Eur. J.* **2009**, *15*, 1310. (d) Lee, J.; Chang, H.; Kim, S.; Bang, G. S.; Lee, H. *Angew. Chem., Int. Ed.* **2009**, *48*, 8501. (e) Guo, Z. Q.; Zhu, W. H.; Shen, L. J.; Tian, H. *Angew. Chem., Int. Ed.* **2007**, *46*, 5549. (f) Baron, R.; Onopriyenko, A.; Katz, E.; Lioubashevski, O.; Willner, I.; Sheng, W.; Tian, H. *Chem. Commun.* **2006**, 2147.
(10) (a) Lee, S. H.; Jung, Y.; Agarwal, R. *Nat. Nanotechnol.* **2007**, *2*, 626. (b) Lankhorst, M. H. R.; Ketelaars, B.; Wolters, R. A. M. *Nat. Mater.* **2005**, *4*, 347.
(11) (a) Kim, T. W.; Choi, H.; Oh, S. H.; Wang, G.; Kim, D. Y.; Hwang, H.; Lee, T. *Adv. Mater.* **2009**, *21*, 2497. (b) Kang, S. J.; Park, Y. J.; Bae, I.; Kim, K. J.; Kim, H. C.; Bauer, S.; Thomas, E. L.; Park, C. *Adv. Funct. Mater.* **2009**, *19*, 2812. (c) Ling, D. Q.; Song, Y. L.; Lim, S. L.; Teo, E. Y. H.; Tan, Y. P.; Zhu, C.; Chan, D. S. H.; Kwong, D. L.; Kang, E. T.; Neoh, K. G. *Angew. Chem., Int. Ed.* **2006**, *45*, 2947.
(12) (a) de Ruiter, G.; Motiei, L.; Choudhury, J.; Oded, N.; van der Boom, M. E. *Angew. Chem., Int. Ed.* **2010**, *49*, 4780. (b) Li, H.; Xu, Q. F.; Li, N. J.; Sun, R.; Ge, J. F.; Lu, J. M.; Gu, H. W.; Yan, F. *J. Am. Chem. Soc.* **2010**, *132*, 5542. (c) Wang, Y.; Liu, Q.; Long, S.; Wang, W.; Wang, Q.; Zhang, M.; Zhang, S.; Li, Y.; Zuo, Q.; Yang, J.; Liu, M. *Nanotechnology* **2010**, *21*, 045202. (d) Lee, D.; Kim, S. U.; Min, J.; Choi, J. W. *Adv. Mater.* **2010**, *22*, 510. (e) Jung, Y.; Lee, S. H.; Jennings, A. T.; Agarwal, R. *Nano Lett.* **2008**, *8*, 2056.
(13) (a) Poverenov, E.; Li, M.; Bitler, A.; Bendikov, M. *Chem. Mater.* **2010**, *22*, 4019. (b) Sonmez, G. *Chem. Commun.* **2005**, 5251. (c) Sonmez, G.; Sonmez, H. B.; Shen, C. K. E.; Wudl, F. *Adv. Mater.* **2004**, *16*, 1905. (d) Kumar, A.; Welsh, D. M.; Morvant, M. C.; Piroux, F.; Abboud, K. A.; Reynolds, J. R. *Chem. Mater.* **1998**, *10*, 896. (e) Havinga, E. E.; Mutsaers, C. M. J.; Jenneskens, L. W. *Chem. Mater.* **1996**, *8*, 769. (f) Gustafsson-Carlberg, J. C.; Inganäs, O.; Andersson, M. R.; Booth, C.; Azens, A.; Granqvist, C. G. *Electrochim. Acta* **1995**, *40*, 2233. (g) Gustafsson, J. C.; Liedberg, B.; Inganäs, O. *Solid State Ionics* **1994**, *69*, 145. (h) Dietrich, M.; Heinze, J.; Heywang, G.; Jonas, F. *J. Electroanal. Chem.* **1994**, *369*, 87. (i) Pei, Q.; Zuccarello, G.; Ahlskog, M.; Inganäs, O. *Polymer* **1994**, *35*, 1347.
(14) For a review on π-conjugate polymers, see. (a) Beaujuge, P. M.; Reynolds, J. R. *Chem. Rev.* **2010**, *110*, 268. (b) Skotheim, T. A.; Reynolds, J. R. In *Handbook of conducting Polymers*, 3rd ed.; CRC Press: Boca Raton, FL, 2007.
(15) (a) Yang, C.; Cho, S.; Chiechi, R. C.; Walker, W.; Coates, N. E. D.; Moses, D.; Heeger, A. J.; Wudl, F. *J. Am. Chem. Soc.* **2008**, *130*, 16524. (b) Allard, S.; Forster, M.; Souharce, B.; Thiem, H.; Scherf, U. *Angew. Chem., Int. Ed.* **2008**, *47*, 4070.
(16) Kulkarni, A. P.; Tonzola, C. J.; Babel, A.; Jenekhe, S. A. *Chem. Mater.* **2004**, *16*, 4556.
(17) (a) Beaujuge, P. M.; Ellinger, S.; Reynolds, J. R. *Nat. Mater.* **2008**, *7*, 795. (b) Krebs, F. C. *Nat. Mater.* **2008**, *7*, 766. (c) Aubert, P.-H.; Argun, A. A.; Cirpan, A.; Tanner, D. B.; Reynolds, J. R. *Chem. Mater.* **2004**, *16*, 2386.
(18) Seshadri, V.; Padilla, J.; Bircan, H.; Radmard, B.; Draper, R.; Wood, M.; Otero, T. F.; Sotzing, G. A. *Org. Electron.* **2007**, *8*, 367.
(19) (a) Yang, C.; Kim, J. Y.; Cho, S.; Lee, J. K.; Heeger, A. J.; Wudl, F. *J. Am. Chem. Soc.* **2008**, *130*, 6444. (b) Thomson, B. C.; Fréchet, J. M. J. *Angew. Chem., Int. Ed.* **2008**, *47*, 58. (c) Thompson, B. C.; Kim, Y.-G.; McCarley, T. D.; Reynolds, J. R. *J. Am. Chem. Soc.* **2006**, *128*, 12714.
(20) (a) Fei, J. F.; Lim, K. G.; Palmore, G. T. R. *Chem. Mater.* **2008**, *20*, 3832. (b) Sonmez, G.; Sonmez, H. B. *J. Mater. Chem.* **2006**, *16*, 2473.

(21) For another application of a known molecule, see. Ceroni, P.; Bergamini, G.; Balzani, V. *Angew. Chem., Int. Ed.* **2009**, *48*, 8516.
(22) Knuth, D. E. In *The Art of Computer Programming; Numerical Algorithms*, 3rd ed.; Addison-Wesley: Reading, MA, 1997.
(23) (a) Hayes, B. *Am. Sci.* **2001**, 89. (b) Hurst, S. L. *IEEE Trans. Comput.* **1984**, *c-33*, 1160.
(24) The information density in multistate memory is $(N/2)^Z$ times higher than in binary memory, where N is the number of states and Z represents the number digits. Alternatively, the digits required to represent a given number is Ln(2)/ln(N) less than in the binary system.
(25) de Silva, A. P.; Dixon, I. M.; Gunaratne, H. Q. N.; Gunnlaugsson, T.; Maxwell, P. R. S.; Rice, T. E. *J. Am. Chem. Soc.* **1999**, *121*, 1393.
(26) Möller, S.; Perlov, C.; Jackson, W.; Taussig, C.; Forrest, S. R. *Nature* **2003**, 166.
(27) Periyasamy, G.; Levine, R. D.; Remacle, F. *Aust. J. Chem.* **2010**, *63*, 173.

AM1007497